A PARAMETRIC ANALYSIS OF FUEL-CLADDING MECHANICAL INTERACTIONS*

F. J. HOMAN.

Metals and Ceramics Division,
Oak Ridge National Laboratory, Oak Ridge, Tennessee, U.S.A.

ABSTRACT

A detailed description of the treatment of fuel-cladding mechanical interaction employed in the FMODEL code is given. A parametric analysis of the materials properties, fabrication variables, and operating conditions which are important to predicted fuel-cladding mechanical interactions is presented and discussed. It is concluded that uncertainty in the fuel thermal expansion data and creep data at low temperatures is most critical for meaningful design analyses, while the influence of uncertainty in the cladding thermal expansion and small changes in the rate of power increases is relatively minor. Uncertainty in cladding creep does not influence the contact pressures resulting from fuel-cladding mechanical interactions predicted with FMODEL, but is important in predicting the overall cladding damage accumulated during service.

1. INTRODUCTION

Mechanical interaction between fuel and cladding in a metal clad ceramic fuel pin influences substantially the performance of the pin. For example, there is an improvement in thermal conductance across the fuel-cladding gap brought about by contact between fuel and cladding. This results in lower fuel operating temperatures. Also, mechanical interaction increases stresses in the cladding beyond those due to fission gas pressure alone. This causes more permanent deformation of the cladding, and may also result in accelerated void swelling. In pellet fuels, mechanical interaction may result in the formation of ridges in the cladding at pellet interfaces due to nonuniform temperature distributions in the pellets. The presence of ridges can lead to "ratchetting" during cyclic operation and this may accelerate failure in the cladding due to metal fatigue.

A valid analytical description of the fuel-cladding mechanical interaction in an operating fuel pin, based on fabrication data and irradiation conditions, would be quite useful in the design of fuel pins and interpretation of irradiation test results. Accordingly, a computer code called FMODEL is being developed at Oak Ridge National Laboratory to simulate the actual in-reactor operation of stainless-steel-clad $(U,Pu)O_2$ LMFBR fuel pins. It is intended that eventually FMODEL will contain analytical descriptions of all possible thermal,

*Research sponsored by the U.S. Atomic Energy Commission under contract with the Union Carbide Corporation.

mechanical, and chemical phenomena which can influence the performance of an operating fuel pin. Many phenomenological descriptions are already included in the code. Whenever possible these descriptions have been developed from first principles. In other cases empirical models are being used until the phenomena are well understood enough to permit sounder theoretical bases. FMODEL does not attempt to force-fit the integrated predictions to measured performance by means of establishing empirical constants. Individual models are developed on the basis of existing data and experience and inserted into the computer code. Simulated irradiation histories are prepared for test pins that have been or will be irradiated and examined. Predicted performance is then compared with measurements made both during and after irradiation of the test pins. If agreement is good the individual models are considered to be adequate. If agreement is not good the reason is sought in faulty fabrication and irradiation conditions, erroneous assumptions, or important phenomena which have been omitted from consideration.

The aspects of FMODEL which deal with fuel-cladding mechanical interaction will be discussed in this work. In addition, a parametric analysis will be presented to demonstrate the sensitivity of predicted mechanical interaction to materials properties of the fuel and cladding, fabrication parameters, and operating conditions.

2. DESCRIPTION OF THE MECHANICAL INTERACTION MODEL

A solid pellet fuel form is the most likely for LMFBR application. Normally there is a fabricated diametral gap between the pellet and cladding of at least 0.001 in. Powdered and spherical fuel forms are also possibilities for the LMFBR and of course with these forms there is no fabricated gap. However, the thermal expansion of nonpellet fuel forms occurs somewhat differently than with pellets, and only pellet fuel forms will be considered here.

When a fuel pin is inserted into a reactor and brought to power, both fuel and cladding thermally expand. The cladding thermal expansion coefficient is higher than that of the fuel at temperatures below 1000°C, so at low heat rates the cladding expands more than the fuel and the fabricated fuel-cladding gap grows. But at high heat rates both fuel temperatures and thermal expansion coefficients increase, and fuel thermal expansion overtakes that of the cladding, causing the gap to grow smaller.

If the fabricated fuel-cladding gap is small and the fuel pin is operated at a sufficiently high heat rate, the fuel will expand thermally to the cladding inner surface. A pressure will develop at the fuel-cladding interface causing both fuel and cladding to creep to relieve the resulting stresses. Calculating the response of a cylindrical cladding tube to a pressure loading at its inner diameter is fairly straightforward, but determination of the response of the fuel cylinder to a pressure at its outer surface is somewhat more complicated.

2.1 Fuel Cracking Model

Typical coolant temperatures in an LMFBR range from 400 to 600°C. A typical fuel pin contains oxide pellets clad in 0.25-in.-OD X 0.015-in.-thick stainless steel tubing. Such a pin operated at moderate heat rates (in the vicinity of 16 kW/ft) will have center temperatures approaching the melting point of the fuel. This causes a wide range of fuel properties across the diameter of the pellet. The fuel at the center is very hot and plastic and is not capable of supporting stresses. The fuel near the cladding is relatively cool and cannot be

strained plastically in tension without cracking. The temperature gradient is very steep, resulting in a high stress gradient across the pellet diameter. If one calculates the stresses based on a homogeneous elastic cylinder, it becomes obvious that stresses of that level cannot be supported. The tensile stresses calculated at the outer fuel fibers exceed the fracture stress and the hot plastic fuel at the pellet center cannot support the high compressive stresses calculated there. This set of conditions is described analytically by assuming radial cracks form in the cold fuel adjacent to the cladding, relieving the thermal stresses in the pellet. The radial cracks extend from the pellet surface to the point where the tensile hoop stress in the pellet exceeds the rupture modulus. The radial position of the root of the crack is determined analytically by comparing the calculated radial distribution of tangential stresses with published rupture modulus values. A graphical illustration of this technique is shown in Fig. 1 where the pellet stress distributions at different heat rates are plotted over rupture modulus curves published by Roberts [1]. It is assumed that the hot plastic core of the pellet, interior to the root of the radial cracks, creeps in response to pressures transmitted from the fuel-cladding interface to the surface of the plastic core by the wedges of cold, cracked fuel exterior to the plastic core.

2.2 Calculation of the Fuel-Cladding Contact Pressure

During initial startup of a fuel pin it is assumed that the time rate of change of linear heat rate is constant. The duration of the power ramp is divided into a number of time steps, Δt. During each Δt, the heat rate of the pin will change by ΔQ. Thermal expansion will cause a change in the outer fuel diameter (ΔD_f) and the cladding inner diameter (ΔD_c). The size of the new fuel-cladding diametral gap is given by

$$\Delta = G_o + \Delta D_c - \Delta D_f \ , \tag{1}$$

where G_o is the gap size at the beginning of the time step. If the calculated gap size (Δ) at the end of the time step is negative, this indicates that the fuel-cladding gap closed during the time step, and mechanical contact exists between the fuel and cladding. To calculate the magnitude of the contact pressure, an iterative scheme is used whereby the existing contact pressure at the beginning of the time step (fission gas pressure in this case) is repeatedly doubled until the correct contact pressure range is bracketed. Then the bracket is repeatedly halved until the contact pressure is within 1% of the previously calculated value. The basis of the iteration is the amount of displacement of the cladding inner diameter and fuel outer diameter due to creep in response to the contact pressure. During a period of time, Δt, the cladding inner diameter will increase by an amount, Δ_c, in response to the pressure. During the same period of time the fuel outer diameter will decrease by an amount, Δ_f, due to the pressure transmitted from the fuel-cladding interface by the cooler cracked fuel to the surface of the hot plastic core. Thus, when the relation

$$\Delta_c + \Delta_f = -\Delta \tag{2}$$

is satisfied, the contact pressure used to calculate Δ_c and Δ_f represents the average contact pressure during the time step. The same procedure is used to calculate the contact pressure during an increase in fuel pin heat rate. However, during steady-state operation the effect of fuel swelling must be considered. The assumption is made that swelling and thermal expansion which occur in the hot plastic core cannot cause radial forces to be transmitted to the cladding. Very little restraint on the plastic core is required to prevent radial movement

of this region, and all swelling in this zone is accommodated axially. However, it is assumed that the cold outer fuel region swells isotropically. Thus, during steady-state operation the ΔD_f term in Eq. (1) is not due to thermal expansion, but to fission product swelling in the cold, cracked fuel region.

3. SENSITIVITY ANALYSIS

A fictitious fuel pin having a fuel-cladding diametral gap of 0.002 in. was established to study the sensitivity of the fuel-cladding mechanical interaction to variations in assumed fuel and cladding properties, fabrication parameters, and operating conditions. The characteristics of this pin are given in Table I. As indicated in the table, the simulated irradiation history for this pin consists of a rise to normal power, a power increase, and an extended period of steady-state operation at normal power. A plot of the predicted (with FMODEL) fuel-cladding mechanical interaction during this irradiation history is given in Fig. 2. Both annealed and 20% cold-worked type 316 stainless steel claddings were considered.

The mechanical interaction is described in terms of the contact pressure at the fuel-cladding interface. The lower portion of the figure shows the predicted buildup of pressure due to differential thermal expansion during power changes and the upper portion is the contact pressure due to fuel swelling during steady-state operation. The predicted contact pressure builds rapidly during power increases, after the initial gap has closed. When normal power has been achieved and the power is no longer increasing, the contact pressure decays as fuel and cladding creep. The same situation prevails during the power increase. The return to normal power from the overpower condition (at about 211-hr elapsed time) is accompanied by a reopening of the fuel-cladding gap because of the reduction in fuel temperatures. This gap gradually closes again due to fuel swelling, but the contact pressures predicted from this source are small compared with those which developed due to power changes early in the irradiation lifetime. For this reason the sensitivity analysis will deal only with the first 200 hr of the irradiation history.

Note that the contact pressures plotted in Fig. 2 for annealed and 20% cold-worked claddings are nearly identical, except during the last 6000 hr or so. This small difference is due to the different swelling characteristics assumed for the two claddings. The similarities early in the irradiation history (in spite of the different creep characteristics of the two claddings) are due to greater sensitivity of contact pressure to fuel creep properties than to those of the cladding. This will be discussed in greater detail later.

3.1 Fuel Thermal Expansion

Examination of the available data for thermal expansion of mixed oxide fuel leaves one somewhat confused. NUMEC investigators have reported that the coefficient of thermal expansion for mixed oxide systems generally increases with increasing plutonium content [2] and decreases with increasing oxygen-to-metal ratio [3]. Equations relating the coefficient of thermal expansion to temperature for several compositions studied by Roth and Halteman [2] are plotted in Fig. 3. Also plotted are the expressions for thermal expansion used in the FMODEL code, based on data for UO_2 and the expression used in the LIFE code [4]. Examination of these plots reveals that the thermal expansion is greater for the 5% Pu compound than for the 12.5% Pu compound (curves 5 and 6). Both compounds have about the same oxygen-to-metal ratio. This contradicts the observation of increasing thermal expansion with increasing

plutonium content for mixed oxides. Two UO_2 samples were measured by Roth and Halteman with slightly different oxygen-to-uranium ratios. Their thermal expansion characteristics were similar (curves 3 and 4). However, two PuO_2 samples were measured, one prepared by oxalate precipitation and the other prepared by hydroxide precipitation, and their thermal expansion characteristics were vastly different (curves 8 and 9).

Since there is substantial variation in the oxygen-to-metal ratios of the compounds studied by Roth and Halteman, little can be concluded from the curves shown in Fig. 3. However, subsequent work by Roth et al. [3] suggests that the following equation describes the change in thermal expansion coefficient of $(U\text{–}20\%\ Pu)O_2$ over the temperature range 0 to 1500°C.

$$\alpha_f = (125.9 - 57.3\ X) \times 10^{-6}\ °C^{-1}\ , \qquad (3)$$

where X is the oxygen-to-metal ratio. The range of applicability of this equation is from oxygen-to-metal ratios of 1.930 to 2.020. According to Eq. (3) the expansion coefficient for stoichiometric $(U\text{–}20\%\ Pu)O_2$ for 0 to 1500°C is about $11.3 \times 10^{-6}\ °C^{-1}$. However, the expression plotted in Fig. 3 for $(U\text{–}20\%\ Pu)O_2$ with an oxygen-to-metal ratio of 2.1 is about $23 \times 10^{-6}\ °C^{-1}$, and from Eq. (3) the thermal expansion coefficient should decrease with increasing oxygen-to-metal ratios. These two results are clearly contradictory. In addition, a single data point for stoichiometric $(U\text{–}20\%\ Pu)O_2$ measured by BNWL investigators [5] is substantially lower than would be predicted from Roth and Halteman's expression for $(U\text{–}20\%\ Pu)O_2$.

The correct expression for thermal expansion coefficient versus temperature for a fuel of a given stoichiometry and plutonium content is not obvious from the available data. However, using an equation of the form

$$\alpha_f = [8 + B(0.00107)\ T] \times 10^{-6}\ °C^{-1}\ , \qquad (4)$$

and varying B between 1.0 and 10.0 yields an envelope which includes most of the curves plotted in Fig. 3. The fuel-cladding mechanical interaction predicted with the FMODEL code, using Eq. (4) with the B values given above to represent the lower and upper boundaries of the envelope, are shown in Fig. 4. The values of the cladding thermal expansion coefficient (α_c) used in this calculation are also given on Fig. 4. The very substantial difference between the predicted behavior of the pin using fuel thermal expansion data from the two extremes of the data envelope indicate that the uncertainty in the thermal expansion characteristics of mixed oxide fuels are not acceptable for design analysis of fuel pins with small fuel-cladding gaps and operated at moderate to high heat rates.

As indicated in Fig. 4, the initial diametral gap was taken as 1 mil, in spite of the fact that the base case value was 2 mils. No fuel-cladding mechanical interaction was predicted by FMODEL with B = 1 and an initial 2-mil gap. To be consistent, the cladding thermal expansion analysis (which follows) was conducted with a 1-mil gap, but all the remaining portions of the sensitivity analysis (except for the gap size analysis itself) use an initial gap size of 2 mils. In addition, all remaining portions of the sensitivity analysis use a value of B = 6 to describe the fuel thermal expansion characteristics.

3.2 Cladding Thermal Expansion

The cladding thermal expansion data are somewhat more consistent than those of the fuel. Figure 5 is a plot of the coefficient of linear thermal expansion versus temperature from

several sources [6–9] for AISI type 316 stainless steel. The data appear to converge at high temperature, and the relatively large divergence at low temperature is of little consequence because cladding temperatures normally are in excess of 400°C. As was the case with the analysis of fuel thermal expansion, predicted fuel-cladding mechanical interactions were computed with the FMODEL code using the upper and lower portions of the data envelope. These results are plotted in Fig. 6. As shown, there is little change in the predicted performance in going from the maximum to the minimum cladding thermal expansion.

3.3 Initial Gap Size

It is logical to expect that fuel-cladding mechanical interaction due to differential thermal expansion between fuel and cladding during power increases would depend strongly upon the size of the fabricated fuel-cladding gap. A large gap provides more space into which the fuel may expand, and this should reduce the interaction. The extent of fuel-cladding interactions for initial cold diametral gaps of 1, 2, and 3 mils is shown in Fig. 7. For these calculations the power density for the cases of 1- and 3-mil gaps was altered to obtain the same heat rates (Table I) that were used for the case with a 2-mil gap. The predicted fuel-cladding mechanical interaction did indeed decrease substantially with each 1-mil increase in the gap size.

3.4 Fuel and Cladding Creep Strength

The creep strength of the fuel material varies with temperature, porosity, stoichiometry, grain size, plutonium and impurity content, and method of fabrication. In addition, the type of test (compressive or bend), test atmosphere, strain rate, rate of fissioning (for in-reactor tests), and prior history of the material will influence the results. The situation is similarly complicated for the cladding. Due to the complex nature of this mechanical property and the vast quantities of data available in the literature, a comprehensive evaluation of the data, such as was done with the thermal expansion data, is beyond the scope of this work. To examine the sensitivity of fuel-cladding mechanical interactions to changes in the creep properties of the fuel and cladding, representative data were selected from the literature and cases run through FMODEL where the creep strengths of fuel and cladding were both increased and decreased by an order of magnitude from base case values. Bohaboy's data [10] for UO_2 (out of reactor) were used for the fuel, and Biancheria's equations [11] were used to describe the thermal creep behavior of type 316 stainless steel cladding, with Claudson's equation [12] to account for flux enhancement of cladding creep.

The changes caused by varying the cladding creep strength an order of magnitude in each direction from the base case values were so slight that they cannot be detected in a plot of contact pressure versus time. The influence of changes in the fuel creep strength is substantial, however, as shown in Fig. 8. Increasing the creep strength (creep rate factor of 0.1) caused the fuel-cladding contact pressure to reach a slightly higher value during both the initial startup and power increase, and to decay much more slowly during the following periods of steady-state operation. Decreasing the creep strength had the reverse effect.

The conclusion which is drawn from these results is that the fuel creep strength controls fuel-cladding mechanical interactions. Thus, it would appear that reducing the uncertainty associated with fuel creep data is more important, from a design standpoint,

than similar effort for the cladding. However, it should be pointed out that, although the plot of fuel-cladding contact pressure versus time changes very little with creep strength of the cladding over two orders of magnitude variation, the total amount of creep predicted from the cladding does indeed change. Since cladding damage is associated in some way with the amount of plastic strain accumulated during service, it is important to have well-characterized cladding as well as fuel, for design purposes.

3.5 Coolant Temperature

The influence of coolant temperature on fuel-cladding interaction for the fictitious pin is shown in Fig. 9. The base case coolant temperature is 500°C. A coolant temperature of 370°C corresponds to the inlet of the EBR-II core, and is also the lowest temperature which can be handled by the "theta" cladding swelling equation [12]. A coolant temperature of 600°C corresponds to the top of the pin. Less mechanical interaction occurs with the higher coolant temperature because the cladding expands thermally more than at the lower temperatures, and both fuel and cladding have less creep strength.

3.6 Rate of Power Increase

To study the influence of the rate of power increase, the duration of the first cycle was first increased to 20 hr, and then decreased to 5 hr. The base case value was 10 hr. Since the heat rate increases from 0 to 16 kW/ft during the first cycle, changing the duration of the cycle effectively changes the slope of the power ramp. The results are shown in Fig. 10. The contact pressure versus time curve is shifted according to the change in the duration of the first cycle, but the magnitude of the contact pressure is influenced very little. It is thus concluded that small changes in the rate of rise to power have little influence on the performance of the pin.

4. DISCUSSION AND SUMMARY

A detailed description of the FMODEL treatment of fuel-cladding mechanical interactions has been given, with a sensitivity analysis of several important materials properties, fabrication variables, and operating conditions which strongly influence mechanical interactions. The influence of changes in these parameters on the fuel-cladding mechanical interaction predicted with FMODEL has been shown graphically. While the plots of fuel-cladding contact pressure versus time are important in understanding the behavior of the small gap, high density pin studied, they do not tell the whole story. It is also important to have some feel for the amount of damage done to the cladding in each case. Using the plastic strain predicted by FMODEL at the outer cladding surface as a measure of cladding damage, the influence of the different parameters can be directly compared. This information is summarized in Table II. If the ratios of the two numbers given for each parameter for each cycle in the operating history are computed and compared, the results are not particularly surprising in view of what has been presented already. The uncertainty in the fuel thermal expansion data produces by far the greatest amount of uncertainty in cladding damage. The range of fuel creep strengths studied has substantial influence on the shape of the fuel-cladding mechanical interaction curve as shown in Fig. 8, but its influence on cladding damage is quite small, as shown in Table II. The entries in Table II dealing with coolant temperature, cladding creep strength, and initial gap size also have fairly large cladding

damage ratios. However, the coolant temperatures studied do not represent uncertainty, but rather the range of temperatures which can be expected along a typical LMFBR fuel pin. That significantly more damage is predicted by FMODEL at the hot end of such a pin than at the cold end, holding everything else constant, is not particularly surprising. The strong influence of initial gap size on mechanical interaction and resulting cladding damage has already been demonstrated in Fig. 7, and the cladding creep strength is being used directly as a measure of cladding damage. Therefore, the fact that a hundredfold change in the creep strength results in significant changes in predicted cladding strain is expected. All the other parameters included in Table II show very little influence on cladding damage, and are therefore concluded to be unimportant, or adequately characterized.

REFERENCES

[1] J.T.A. Roberts and B. J. Wrona, "Plastic Yielding and Fracture of Mixed Oxides," Reactor Development Program Progress Report, USAEC Report ANL-7737, pp. 129–130, Argonne National Laboratory, August 1970.

[2] J. Roth and E. K. Halteman, Thermal Expansion of Coprecipitated $(U,Pu)O_2$ Powders by X-Ray Diffraction Techniques, USAEC Report NUMEC-2389-9, Nuclear Materials and Equipment Corp., October 1965.

[3] J. Roth et al., "The Effects of Stoichiometry on the Thermal Expansion of 20 w/o PuO_2-UO_2 Reactor Fuel," Trans. Am. Nucl. Soc. 10(2), 457 (1967).

[4] V. Z. Jankus and R. W. Weeks, LIFE-I, A Fortran IV Computer Code for the Prediction of Fast-Reactor Fuel-Element Behavior, USAEC Report ANL-7736, Argonne National Laboratory, November 1970.

[5] R. P. Nelson, "Thermal Expansion of Mixed UO_2-PuO_2," Quarterly Progress Report, April, May, June, 1967, Reactor Fuels and Materials Development Programs for Fuels and Materials Branch of USAEC Division of Reactor Development and Technology, USAEC Report BNWL-473, p. 4.1, Battelle-Northwest.

[6] Metals Handbook, Vol. 1, Properties and Selection of Metals, 8th ed., p. 423, American Society for Metals, Metals Park, Ohio, 1961.

[7] Working Data, Carpenter Stainless and Heat Resisting Steels, Selection, Description, Fabrication, The Carpenter Steel Company, Reading, Pennsylvania, 1962.

[8] B. J. Seddon, Steels Data Manual, TRG Report 840, Technical Research Group, 1965.

[9] I. B. Fieldhouse, J. C. Hedge, and J. I. Lang, Measurements of Thermal Properties, WADC-TR-274, Wright Air Development Center, 1958.

[10] P. E. Bohaboy, R. R. Asamoto, and A. E. Conti, Compressive Creep Characteristics of Stoichiometric Uranium Dioxide, USAEC Report GEAP-10054, General Electric Company, May 1969.

[11] A. Biancheria et al., "Analysis of Secondary Creep Rate Data for Type 316 SS," Oxide Fuel Element Development Quart. Progr. Rept. Sept. 30, 1969, USAEC Report WARD-4135-1, p. 19, Westinghouse Electric Corp.

[12] T. T. Claudson, Irradiation Induced Swelling and Creep in Fast Reactor Materials, USAEC Report BNWL-SA-3283, Battelle-Northwest, May 1970.

Table I. Fabrication Data and Operating Conditions for Base Case Fuel Pin[a]

Cladding outside diameter, in.	0.25
Cladding thickness, in.	0.015
Fuel pellet diameter, in.	0.218
Fuel density, % of theoretical	95
Normal power, kW/ft	16
Overpower, kW/ft	17.6
Flux (normal power), neutrons cm^{-2} sec^{-1} (> 0.1 MeV) × 10^{15}	1.53
Fluence, neutrons/cm^2 (> 0.1 MeV) × 10^{22}	6.73
Coolant temperature, °C	500
Burnup, % FIMA	12.75
Gap conductance between fuel and cladding, W cm^{-2} $°C^{-1}$	1.136
Film conductance between cladding and sodium, W cm^{-2} $°C^{-1}$	11.36

[a]Operating history: The pin is brought to normal power over 10 hr and held for 100 hr. Then the power is increased to a 10% overpower condition over 1 hr and held for an additional 100 hr. The pin is then lowered to normal power and operated under steady-state conditions for 12,000 hr.

Table II. Summary of Accumulated Plastic Strains

Case	Cumulative Cladding Plastic Strain at End of Cycle,[a] %				
	1	2	3	4	5
Base case					
Annealed cladding	1.64×10^{-4}	1.17×10^{-3}	1.19×10^{-3}	2.45×10^{-3}	1.84×10^{-2}
20% cold-worked cladding	1.12×10^{-4}	8.86×10^{-4}	8.97×10^{-4}	1.78×10^{-3}	1.27×10^{-1}
Fuel thermal expansion					
B = 10	2.63×10^{-2}	3.66×10^{-2}	3.67×10^{-2}	3.97×10^{-2}	
B = 1	3.01×10^{-5}	5.54×10^{-4}	5.61×10^{-4}	1.22×10^{-3}	
Cladding thermal expansion					
C = 18 D = 0.00308	8.99×10^{-5}	8.85×10^{-4}	9.07×10^{-4}	1.86×10^{-3}	
C = 14 D = 0.00615	1.50×10^{-4}	1.01×10^{-3}	1.03×10^{-3}	2.04×10^{-3}	
Fuel creep rate					
Factor = 0.1	2.01×10^{-4}	3.11×10^{-3}	1.18×10^{-2}	1.46×10^{-2}	
Factor = 10	5.92×10^{-5}	6.17×10^{-4}	6.37×10^{-4}	1.52×10^{-3}	
Cladding creep rate					
Factor = 0.1	1.64×10^{-5}	1.19×10^{-4}	1.21×10^{-4}	2.47×10^{-4}	
Factor = 10	4.40×10^{-4}	9.38×10^{-4}	9.66×10^{-4}	1.12×10^{-3}	
Coolant temperature					
370°C	8.60×10^{-5}	1.26×10^{-3}	1.28×10^{-3}	2.62×10^{-3}	
600°C	1.43×10^{-2}	6.32×10^{-2}	6.56×10^{-2}	1.70×10^{-1}	
Rate of power increase					
Doubled	4.74×10^{-5}	1.11×10^{-3}	1.12×10^{-3}	2.39×10^{-3}	
Halved	3.28×10^{-4}	1.26×10^{-3}	1.27×10^{-3}	2.54×10^{-3}	
Initial gap size					
1 mil	3.72×10^{-3}	7.57×10^{-3}	7.75×10^{-3}	9.00×10^{-3}	2.69×10^{-2}
3 mils	3.75×10^{-5}	7.09×10^{-4}	7.18×10^{-4}	1.61×10^{-3}	1.76×10^{-2}

[a]Cycle 1 – rise to full power over 10 hr; cycle 2 – steady-state operation at full power for 100 hr; cycle 3 – power increase to 10% overpower over 1 hr; cycle 4 – steady-state operation at 10% overpower for 100 hr; cycle 5 – steady-state operation at 16 kW/ft for 12,000 hr.

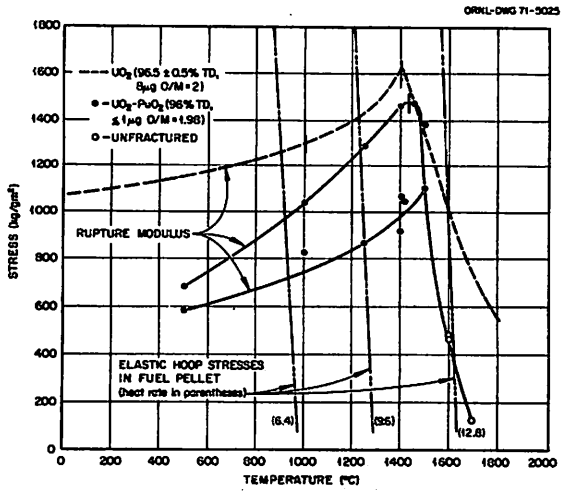

Fig. 1. Rupture Modulus Versus Temperature for UO_2 and $(U,Pu)O_2$.

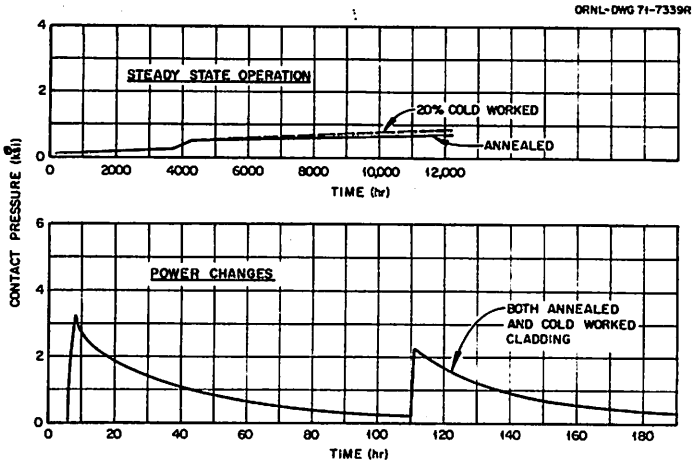

Fig. 2. Influence of Cladding Cold Work on Fuel Cladding Mechanical Interaction.

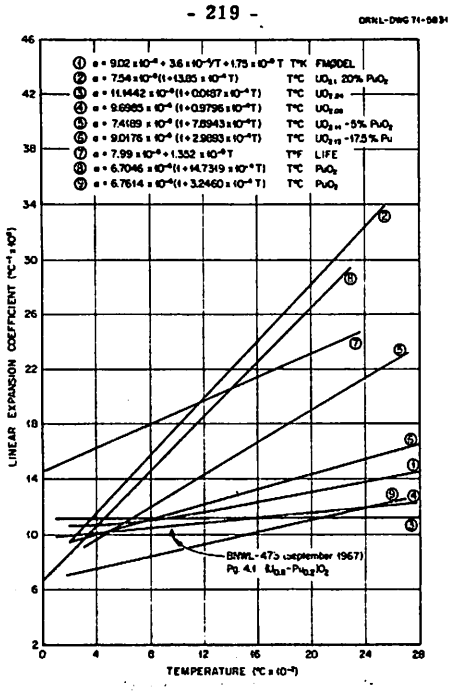

Fig. 3. Thermal Expansion Coefficient Versus Temperature for Mixed Oxide Fuels.

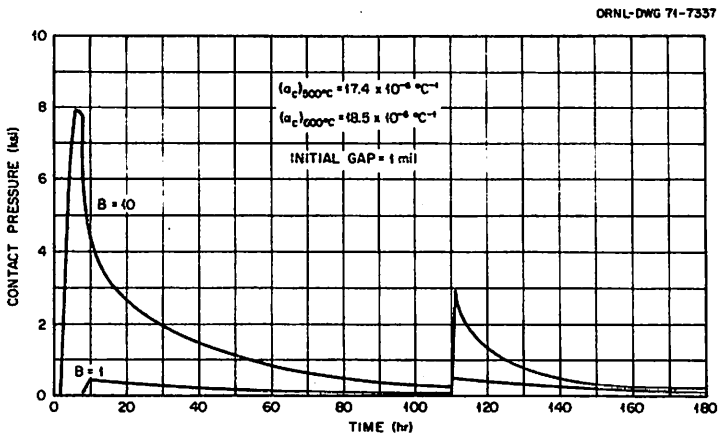

Fig. 4. Influence of Uncertainty in Fuel Thermal Expansion Characteristics on

Mechanical Interaction.

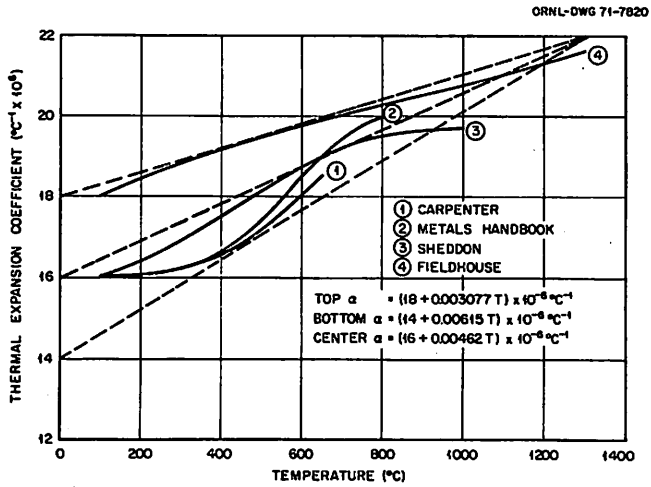

Fig. 5. Thermal Expansion Coefficient Versus Temperature for Type 316 Stainless Steel.

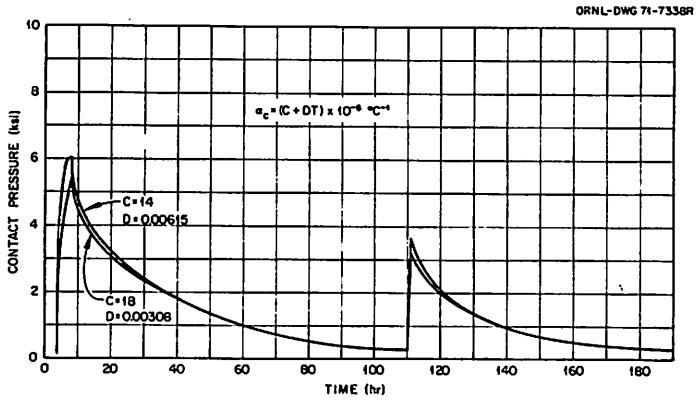

Fig. 6. Influence of Uncertainty in Cladding Thermal Expansion Characteristics on

Mechanical Interaction.

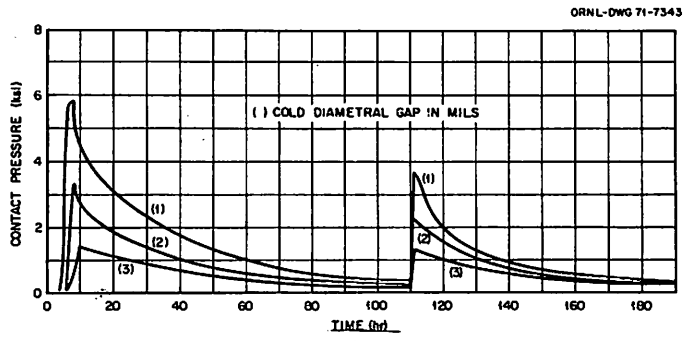

Fig. 7. Influence of Initial Gap Size on Predicted Mechanical Interaction.

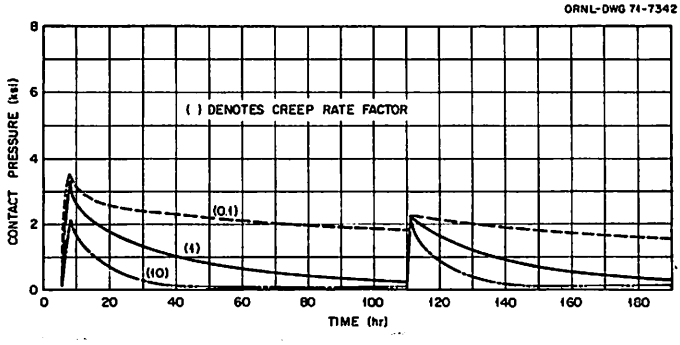

Fig. 8. Influence of Fuel Creep Strength on Predicted Mechanical Interaction.

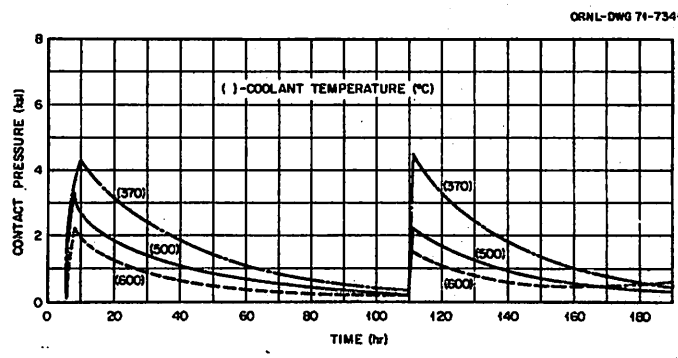

Fig. 9. Influence of Coolant Temperature on Predicted Mechanical Interaction.

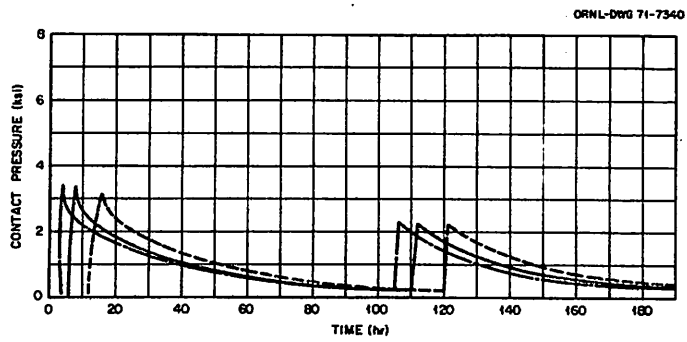

Fig. 10. Influence of Slope of Power Ramp on Predicted Mechanical Interaction.